Innov Biosyst Bioeng, 2025, vol. 9, no. 4, 28–45
doi: 10.20535/ibb.2025.9.4.347453

Original article

COMPARATIVE ASSESSMENT OF CYTOTOXICITY OF ALIPHATIC AMINO CARBOXYLIC COMPOUNDS AS POTENTIAL ANTICORONAVIRUS AGENTS

M.P. Smetiukh[1*], A.S. Momot[1], O.P. Trokhimenko[2], S.O. Soloviov[1,2], I.S. Datsenko[2], O.K. Yakovenko[3,4], Y.O. Dziublyk[5], O.V. Kozyr[1], M. S. Hakim[6]

[1] Igor Sikorsky Kyiv Polytechnic Institute, Kyiv, Ukraine
[2] Shupyk National University of Health Care of Ukraine, Kyiv, Ukraine
[3] Municipal Enterprise "Volyn Regional Clinical Hospital", Lutsk, Ukraine
[4] Lesya Ukrainka Volyn National University, Lutsk, Ukraine
[5] F. G. Yanovskyi National Scientific Center of Phthisiology, Pulmonology and Allergology of the National Academy of Medical Sciences of Ukraine, Kyiv, Ukraine
[6] College of Medicine, Qassim University, Buraydah, Saudi Arabia

*Corresponding author: mykhailo.smetiukh@lll.kpi.ua

Received 25 July 2025; Accepted 2 December 2025

Background. Despite the success in creating vaccines against SARS-CoV-2, the high mutagenicity of coronaviruses, interspecies transmission, and the emergence of new strains require further search for effective antiviral agents. A key step in this process is to evaluate the cytotoxicity of potential compounds to determine their safety and therapeutic potential. Modern IT solutions, such as automated image analysis and artificial intelligence, increase the accuracy and objectivity of assessments.
Objective. To determine the cytotoxicity of compounds with potential anticoronavirus activity and to analyze it using IT tools.
Methods. The study used the grafting cell line BHK-21 of the gerbil hamster, which was incubated with seven aliphatic amino carbon compounds in six concentrations. Cell viability was determined using the MTT assay. Cell monolayer image processing and an exponential dose-response model were used for automated analysis.
Results. The study revealed a pronounced dose- and time-dependent cytotoxicity of most samples, with a maximum decrease in viability at concentrations above 10 mg/ml. The hormesis effect was recorded at low concentrations (up to 5–10 mg/ml), which may indicate the activation of cellular defense mechanisms. The high correlation between measurements at 492 nm and 550 nm ($R^2 > 0.98$) confirmed the reliability of the spectrophotometric data. The exponential model allowed us to approximate the toxicity curves, especially in the middle and high concentration ranges. The built neural network based on image data and MTT test showed the ability to predict cell viability even with a limited amount of training data.
Conclusions. The combination of the MTT assay with automated image analysis provides a comprehensive assessment of cytotoxicity. A dose-dependent decrease in cell viability and morphological changes under the influence of the studied compounds were found. Measurements at 550 nm proved to be more sensitive to early changes in cell metabolism. The use of IT algorithms has demonstrated the prospects of an automated approach to the screening of biologically active substances.

Keywords: cytotoxicity*; in vitro*; amino carbon compounds; MTT test; image processing; neural network.

Introduction

Coronaviruses (CoVs) are complex viruses whose genome is represented by single-stranded unfragmented RNA of positive polarity, which got their name because of the morphological features of the virion, whose electron micrograph shows protrusions of surface proteins in the form of a crown. Coronaviruses mainly cause respiratory and intestinal diseases in mammals and birds with varying degrees of severity [1, 2, 3]. The disease outbreaks caused by the SARS-CoV (2002–2003), MERS-CoV (2012) and SARS-CoV-2 (2019) coronaviruses in the last 20 years have demonstrated the high threat of these viruses to global health, which has necessitated the development of new and study of existing medicines for the prevention and treatment of diseases caused by them [4–6].

Despite significant progress in the development of vaccines against SARS-CoV-2, the high level of mutability, the emergence of new variants and the possibility of interspecies transmission of coronaviruses emphasize the need to continue to search for effective antiviral drugs [7–9].

One of the most promising areas of antiviral drug development is the study of low molecular weight compounds, in particular aliphatic amino acids. Aliphatic amino acids are important biologically active molecules that can potentially affect the viral reproduction cycle by inhibiting its individual phases or changing metabolic processes in infected

cells [10–14]. Previous studies have evaluated the antiviral activity of a number of aliphatic amino acids and their derivatives against the prototypical coronavirus strain, IBV infectious bronchitis in chickens, *in vitro*. It was found that some of the studied substances, in particular 4-aminobutyric acid and 6-aminocaproic acid, have promising antiviral effects in non-toxic concentrations and show high values of the chemotherapeutic index (CTI ≥ 4) under different regimens of application [15]. In this research determination of the valid cytotoxicity level is one of the mandatory stages of the antiviral drug finding process [16]. Key method of this stage is the cytotoxicity assay, which allows one to determine the level of influence of a substance on cell viability *in vitro*, which can be measured as the degree of ability of a substance to cause cell damage by disrupting or altering its basic functions [17, 18].

Although cytotoxicity assessment methods are well established, it remains uncertain whether the results of cytotoxicity studies for compounds with potential anti-coronavirus activity will be reproducible under varying experimental conditions – in particular, when changing detection parameters, using different types of equipment, or altering the duration of exposure of the substance to cells. This variability in results may lead to uncertainty in decision-making at subsequent stages of investigating these compounds as potential antiviral agents [19–22].

Nowadays, automated tools based on information technologies based on neural networks are increasingly replacing routine methods of detecting outcomes in biomedical research, potentially offering higher accuracy and simplifying experimental procedures. In particular, modern image processing techniques enable the automated detection of morphological changes in cells and cell monolayers caused by test compounds, significantly reducing the labor intensity and subjectivity of result interpretation [23–25]. Additionally, the use of artificial neural networks opens up possibilities for predicting and assessing compound toxicity both in large datasets and under conditions of limited experimental data [26, 27]. However, it is important to emphasize that such approaches do not represent expert evaluation in the traditional sense but are based on algorithmic decision-making. This raises important concerns regarding model retraining, potential errors, and reproducibility, especially when applying IT tools across different experimental settings or to novel compounds. As a result, the validation of such automated systems against classical methods remains a critical issue for ensuring the reliability and credibility of their outputs.

The aim of the study was to evaluate the consistency and reliability of cytotoxicity assessment results for aliphatic amino acids with potential anti-coronavirus activity under varying experimental conditions and detection approaches, including the use of neural networks.

Materials and Methods

The study used seven aliphatic amino carboxylic acids and their derivatives in six different concentrations: 50, 20, 10, 5, 2.5, and 1.25 mg/ml (Table 1).

As an experimental *in vitro* cell model, the grafted substrate-dependent Syrian hamster kidney cell line BHK-21, obtained from the Museum of Cell Cultures of the R.E. Kavetsky Institute of Experimental Pathology, Oncology and Radiobiology of the National Academy of Sciences of Ukraine (Kyiv), previously adapted for virological studies of substances with potential action against coronaviruses, was used [32].

For cell cultivation, RPMI-1640 medium with L-glutamine and sodium bicarbonate and DMEM with 4500 mg/L glucose, L-glutamine and sodium bicarbonate without pyruvate were used. Rostock medium was prepared by mixing these media in equal proportions with 10% fetal bovine serum and antibiotics (penicillin – 100 U/ml, streptomycin – 100 μg/ml). The maintenance medium contained the same components but without fetal serum. A 0.02% solution of ethylenediaminetetraacetic acid (Versene solution) was used to remove cells from the growth surface.

Cells were cultured in 50 cm^3 polystyrene culture mattresses with a growth surface area of 75 cm^2, as well as in 24- and 96-well cell culture plates with an adhesive surface. Cells were incubated at 37°C in 5% CO_2.

Cytotoxicity testing of the compounds was carried out using 24-hour and 48-hour cell cultures to evaluate the influence of cell maturity on the reproducibility and reliability of the results. Comparisons were made between reference monolayers and monolayers treated with test samples, which provided an interpretation of the cytotoxic effects. The analysis was performed after 24 hours of exposure to the test substances. To identify potential image deviations, treated monolayers were compared with reference monolayers whose cells were not exposed to the test compounds. Lens magnification in all images was ×20.

Most of the methods for assessing *in vitro* cytotoxicity are simple to perform, which ensures their widespread use in the study of biologically active compounds [33, 34]. The cytotoxic effect of these samples was determined by analyzing cell viability using the MTT (3-(4,5-dimethylthiazol-2-yl)-2,5-diphenyltetrazolium bromide) assay in accordance with the instructions for the use of Roshe Cell Proliferation Kit I (MTT). In particular, the MTT assay is currently one of the most common colorimetric methods and is considered a reference method for

Table 1: The studied aliphatic amino carboxylic acids and their physicochemical properties [28–31]

Concentration	The length of the aliphatic chain, å	Number of functional groups	Ionization	Polarity	Solubility	Molecular weight, g/mol
4-amino–butyric acid (T1)	4.62	Amine (-NH_2), carboxylic (-COOH)	pH = 7.2 (10 g/L, H_2O, 21.5°C), pKa = 4.031 (25°C)	The topological area of the polar surface is 63.3 Å^2	Easily soluble in water, slightly soluble in hot ethanol, insoluble in cold ethanol, ether and benzene	103.121
5-aminovaleric acid (T2)	6.16	Amine (-NH_2), carboxylic (-COOH)	pKa = 4.27 (25°C), pH = 7	The topological area of the polar surface is 63.3 Å^2	Solubility in water: 1000 mg/ml (20°C). Solubility order: THF > carbon tetrachloride > ethanol > methanol	117.15
Hydrochloride of 6-amino–caproic acid (T3)	7.70	Amine (-NH_2), carboxylic (-COOH), halogen (Cl-)	pKa = 4.373 (25°C)	The topological area of the polar surface is 63.3 Å^2	-	167.63
8-amino–caproic acid (T4)	10.78	Amine (-NH_2), carboxylic (-COOH)	pKa = 4.89 (25°C)	The topological area of the polar surface is 63.3 Å^2	Solubility in water: 31 mg/ml (20°C)	159.23
7-amino–heptanoic acid (T5)	9.24	Amine (-NH_2), carboxylic (-COOH)	pKa = 4.502 (25°C)	The topological area of the polar surface is 127 Å^2	Soluble in water	145.20
6-amino–caproic acid (T6)	7.70	Amine (-NH_2), carboxylic (-COOH)	pKa = 4.373 (25°C), pH = 7.0-7.5 (50 g/L, H_2O, 20°C)	The topological area of the polar surface is 63.3 Å^2	Solubility in water: 505.0 mg/mL (25°C)	131.17
Methyl-6-aminocaproic hydrochloride (T7)	7.70	Amine (-NH_2), ester (-COO-), halogen (Cl-)	-	The topological area of the polar surface is 52.3 Å^2	Well soluble in water, chloroform (slightly), methanol (slightly)	181.66

assessing cytotoxicity or cell viability [35–38]. It is based on the determination of cell viability by assessing the function of mitochondria, which is assessed by the activity of mitochondrial enzymes, in particular, succinate dehydrogenase [39]. In this test, MTT is reduced to purple formazan by NADH. The resulting product can be quantified by measuring the absorbance of visible light of a specific wavelength [40, 41]. The optical density (OD) of the solution in the wells of the plates was measured using a plate spectrophotometer at two wavelengths of 550 and 492 nm. The cell viability was determined 24 and 48 hours after exposure to the test compounds as a relative decrease in OD compared to the reference. This method is significantly superior to other dye-based methods because it is easy to use, safe, highly reproducible, and widely used to deter-mine both cell viability and cytotoxicity [39, 42].

Traditional approaches to cytotoxicity analysis are based on calculating the difference between the average cell viability values in reference and experimental samples within each concentration of the test substance. The approach we propose extends this concept by identifying all possible options for pairwise comparison between reference and experimental samples. This allows for a better assessment of the real variability of the possible toxic effect, especially when the samples are heterogeneous or contain certain statistical outliers. This approach is especially relevant in cases where the number of replicates within a given concentration is limited, as it eliminates the need to select a specific reference value for comparison. The next step was to determine the average value of the percentage decrease in cell survival, which allowed us to obtain a generalized dose-dependent assessment of cytotoxicity for each specific concentration of the substance. For further analysis of the dose-dependent cellular response to each tested compound, an exponential inhibition model was applied, which is a standard approach in toxicological studies [43]. This model allows us to determine the critical points of exposure to the test substance, in particular, the threshold concentrations and their range, in which the maximum decrease in cell viability is observed:

$$\Delta V(C) = \frac{\Delta V_{max}}{1 + e^{(-S(C-A))}} - \Delta V_0$$

where: $\Delta V(C)$ is the predicted value of the decrease in cell viability, %, ΔV_{max} is a coefficient that determines the maximum decrease in cell viability, C – concentration of the test substance (T1-T7), mg/ml, S is a parameter of curve steepness (sensitivity of the cell system to changes in concentration.

To automate the assessment of changes in the cell monolayer, the self-designed software "CellCalc" was developed using the Python programming language and artificial intelligence methods (Certificate of Copyright Registration No. 131305 dated 12.11.2024). This tool enables automated recognition of cells in microscopic images, counts their number, and estimates parameters such as size, area, and other morphological characteristics compared to a reference sample. For the preliminary evaluation of the cytotoxicity of tested compounds, the Cellpose neural network was integrated into "CellCalc". A classical Feedforward model was chosen as the neural network architecture, consisting of three internal layers of neurons and one output neuron. The number of neurons in the hidden layers was selected experimentally, considering the ratio between the model complexity and the available amount of training data. ReLu was chosen as the activation function of the neurons in the inner layers. The Mean Squared Error (MSE) function was used as a criterion for model quality, which is a standard approach for regression tasks, and the accuracy was evaluated using the Mean Absolute Percentage Error (MAPE).

This model demonstrated high segmentation performance (AP@0.5 = 0.785) during training. Further morphological analysis, including cell count and area estimation, was carried out using algorithms based on the OpenCV library, a powerful tool for image processing and computer vision. The performance of the neural network model largely depends on two key parameters: the average cell size in pixels and the sensitivity threshold for recognition. A lower threshold allows for the detection of more cells but also increases the risk of false positives, where noise or artifacts may be incorrectly identified as cells. Therefore, image processing parameters were adjusted individually, taking into account factors such as image scale, quality, and lighting conditions. Images of the cell layer obtained after treatment with the tested compounds, along with MTT assay results, served as the foundation for training a custom neural network aimed at predicting cell viability. The input dataset included information on the number, size, and area of cells, as well as spectrophotometric indicators.

The model's output was a quantitative prediction of the decrease in cell viability compared to the reference monolayer. Examples of the initial images and the results of automated cell recognition by Cellpose are shown in Fig. 1.

The dataset for neural network training consis-

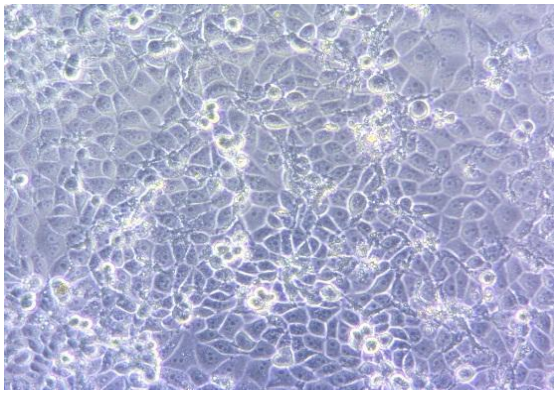

Reference monolayer (x20)

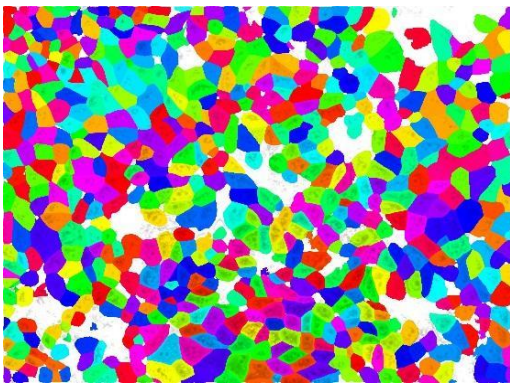

Segmented image of the reference monolayer

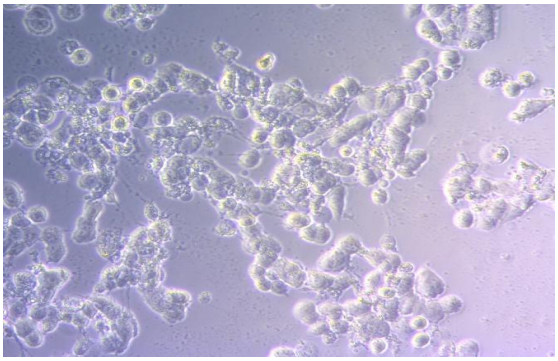

T3, 50 mg/ml (x20)

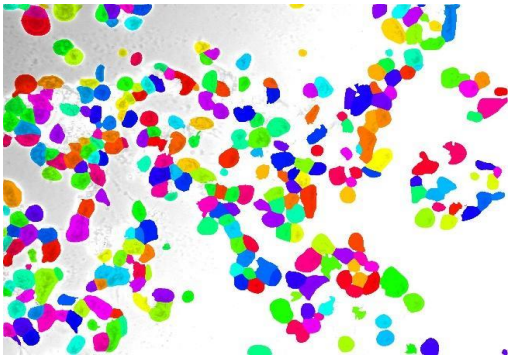

Segmented image of T3, 50mg/ml (x20)

Figure 1: An example of image processing of a cell monolayer

ted of 29 samples. Among them, 24 samples were used for training and 5 for testing. The training data were not divided into mini-batches. The overall size of the training set is substantially limited, since supervised neural network training typically requires at least several hundred samples. An insufficient number of training instances has a markedly negative impact on the performance of the neural network, potentially leading to overfitting or inadequate generalization to new samples.

To solve the prediction task, a fully connected multilayer feedforward neural network was implemented in TensorFlow. The model architecture consists of four sequential layers. The input layer receives a feature vector of dimensionality 5. The first hidden layer contains 200 neurons with ReLU activation and employs L2 regularization (coefficient l2 = 0.01) to reduce overfitting. The second hidden layer contains 50 neurons with ReLU activation. The third hidden layer consists of 8 neurons, also using ReLU activation. The output layer has 1 neuron without an activation function, which corresponds to the formulation of a regression task.

The number of neurons in the hidden layers was selected experimentally, taking into account the balance between model complexity and available training data. The Adam optimizer with a learning rate of 0.0001 was used for training. Mean Squared Error (MSE) was applied as the loss function, which is a standard approach for regression tasks, and accuracy was evaluated using Mean Absolute Percentage Error (MAPE). The neural network was trained for 150 epochs. Due to the small sample size, the validation set was not used, and the results were evaluated only on the test subset. The developed model architecture and its training graph are shown in Fig. 2. As a result of training the neural network model, MSE of 0.12 and MAPE of 25.27% were obtained.

Results

The results of the cytotoxicity study of the test samples allowed us to assess the differences in the registration of changes in the cell monolayer and cell viability at two wavelengths – 492 nm and 550 nm after 24 and 48 hours of exposure. Thus, for the test sample T1, after 24 hours of exposure, the toxic effect is less pronounced with different technologies, indicating possible mechanisms of cell adaptation or insufficient accumulation of the toxic effect of gamma-aminobutyric acid (GABA). After exceeding a certain concentration level (≈10 mg/ml), a sharp decrease in cell viability is observed. The model curves approximate the experimental data well in the medium and high concentration range. However, at low concentrations, deviations between the experiment and the model are observed, which may be due to the variability of the biological response of cells (Fig. 3).

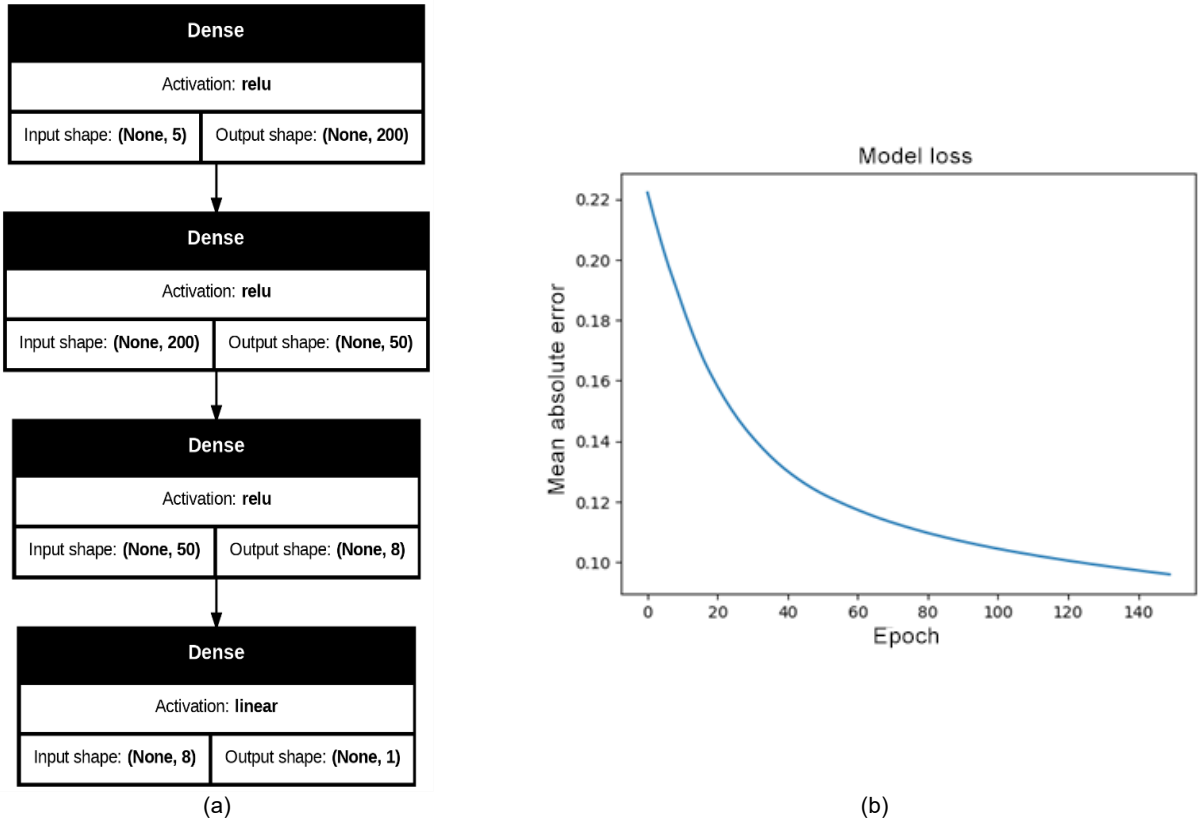

(a) (b)

Figure 2: Architecture (a) and training graph (b) of neural network for cell viability prediction

For the T2 sample, after 24 hours of exposure at low concentrations, a sharp decrease in cell viability is clearly observed, indicating a high sensitivity of the cells to the test compound (Fig. 4). In the range from 10 to 50 mg/ml, the toxodynamics curve becomes more linear at different wavelengths. A stimulating effect at low concentrations (hormesis effect) is observed after 48 hours, as with the T1 sample. However, with increasing concentration, the toxic effect becomes more pronounced. The pronounced nonlinear

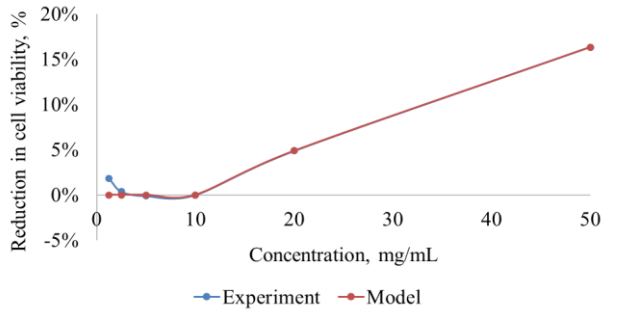

24 hours, 550 nm

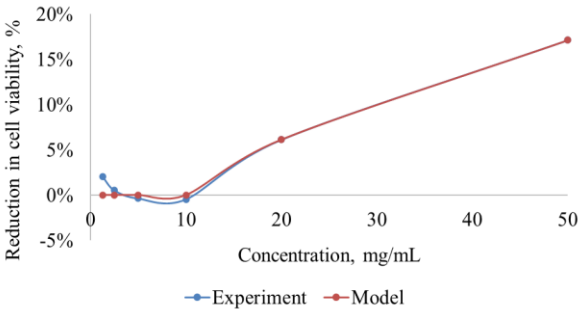

24 hours, 492nm

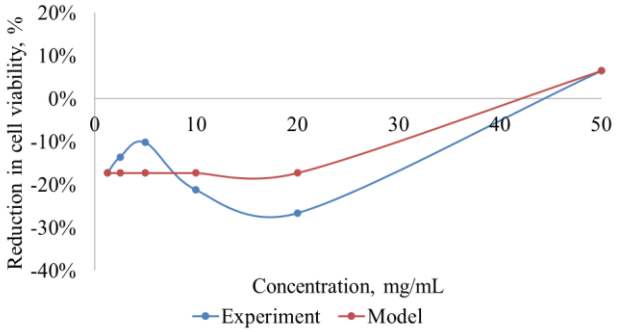

48 hours, 550 nm

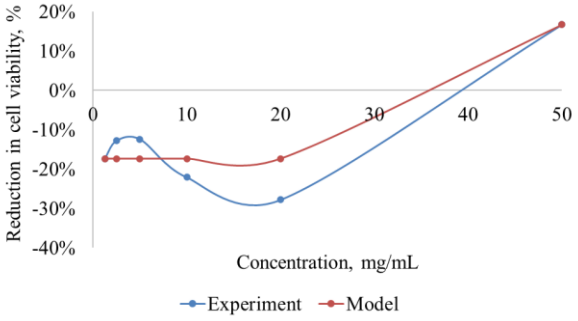

48 hours, 492 nm

Figure 3: Toxicity dynamics for T1

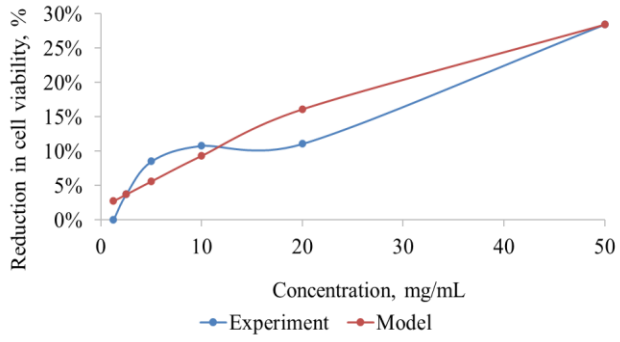

24 hours, 550 nm

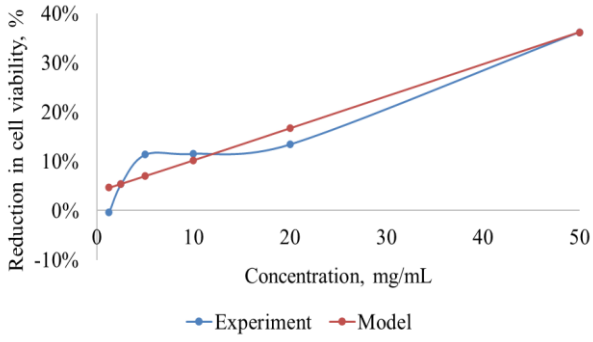

24 hours, 492 nm

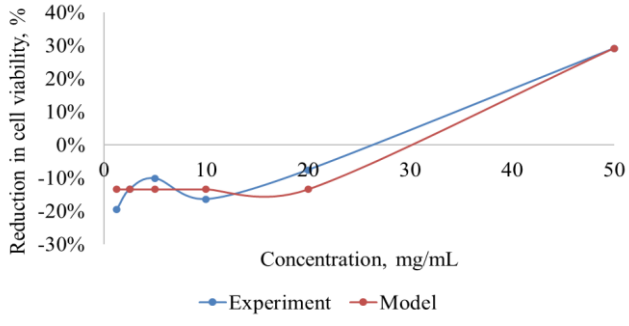

48 hours, 550 nm

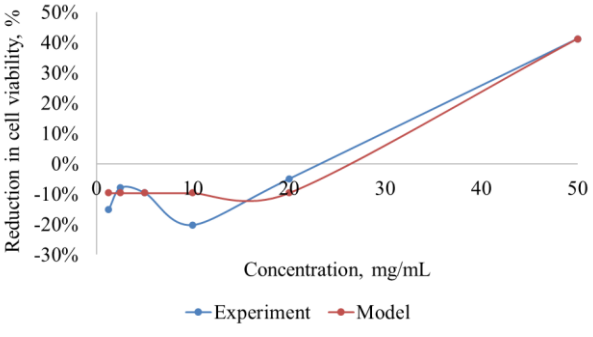

48 hours, 492 nm

Figure 4: Dynamics of T2 toxicity

nature of the dependence of the toxicity of a compound on its concentration is clearly observe at different wavelengths and at different exposure times. Due to the complex mechanisms of interaction between a substance and cells, such as the observed hormesis, it is difficult to approximate the experimental data. Nevertheless, the model reflects the real trend in the toxic effect of T2 on BHK-21 cells.

The toxicodynamics curves for the T3 sample demonstrate a characteristic S-shaped (sigmoid) dependence, which is typical for concentration-dependent toxic effects. It is observed that at concentrations above 10 mg/ml, the curve reaches a plateau of cytotoxic effect, indicating maximum cytotoxicity (Fig. 5).

Comparison of the results at 550 nm and 492 nm indicate their similarity, and the time points demonstrate the consistency of the data obtained. The deviations between the experimental results and the mathematical model are insignificant and occur mainly at high concentrations, which may be due to the saturation effect.

Instead, the model curve for T4 (8-amino-caproic acid) demonstrates a high correspondence to the experimental data at both wavelengths, indicating the stability of the results.

As in the previous cases, the general trend of cell viability decrease depending on the concentration of the substance is dose-dependent, however, with a more pronounced effect at longer exposure. After 48 hours, a more significant decrease in viability was observed, indicating a cumulative cytotoxic effect or gradual depletion of the adaptive mechanisms of BHK-21 cells. At low concentrations (about 5 mg/ml), there is a temporary increase in viability or no pronounced cytotoxic effect, which may be due to the adaptive reactions of cells. This feature becomes more noticeable after 48 hours, which may indicate the activation of compensatory mechanisms in the early stages of T4 exposure (Fig. 6). At higher concentrations, a signifi cant decrease in viability is observed, which is likely caused by accumulation of damage, impaired mitochondrial function, or induction of apoptosis. Thus, 8-aminocaproic acid exhibits time- and dose-dependent toxicity to the HNSCC-21 cell line.

Similar to T4, test sample T5 (7-amino-heptanoicacid) exhibits significant cytotoxicity against HNSC-21 cells, which is dose-dependent and reaches a maximum at concentrations of approximately 10 mg/ml. Further increase in the concentration of the test compound does not lead to significant changes in the cytotoxic effect, indicating that the toxicity plateau has been reached. Increasing the exposure time to 48 hours leads to stabilization of the cytotoxic effect, which may indicate the accumulation of toxicity or depletion of compensatory mechanisms of cells.

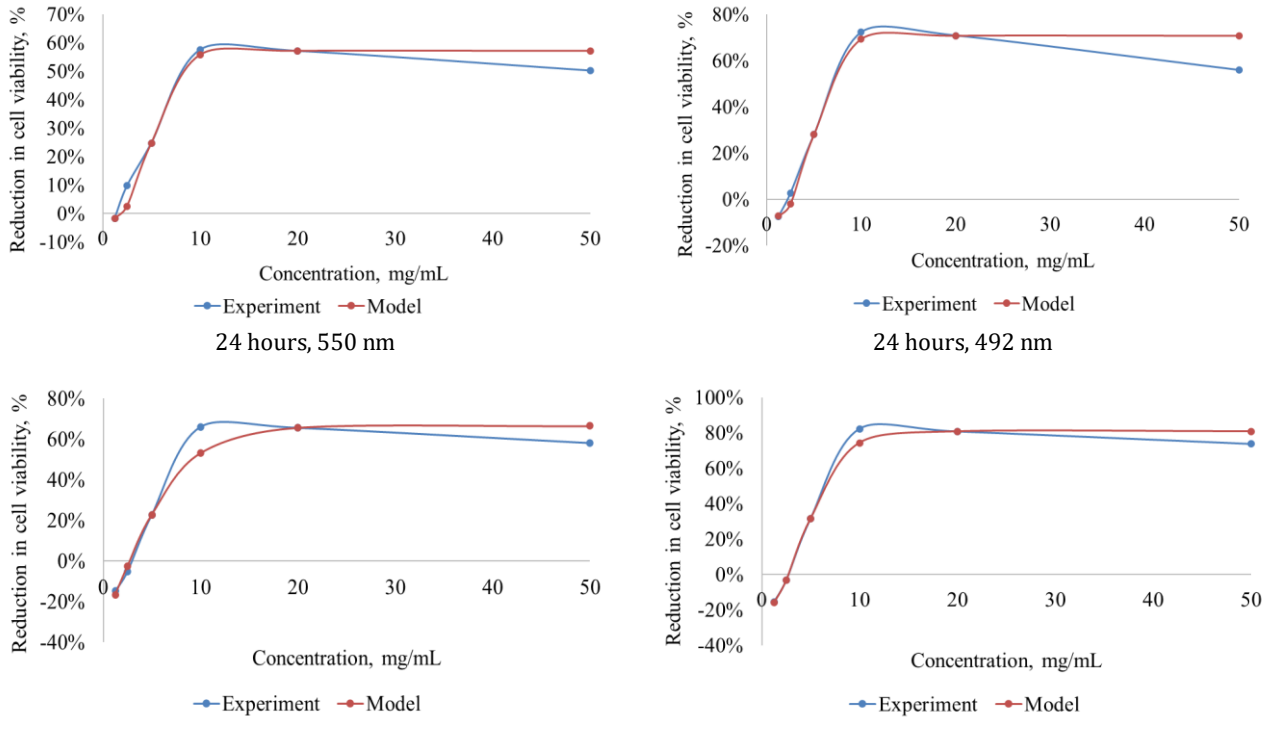

Figure 5: Dynamics of T3 toxicity

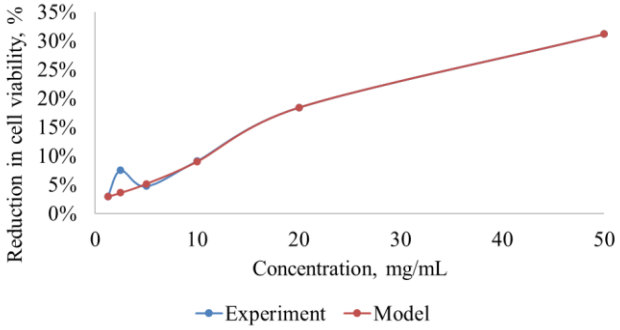

24 hours, 550 nm

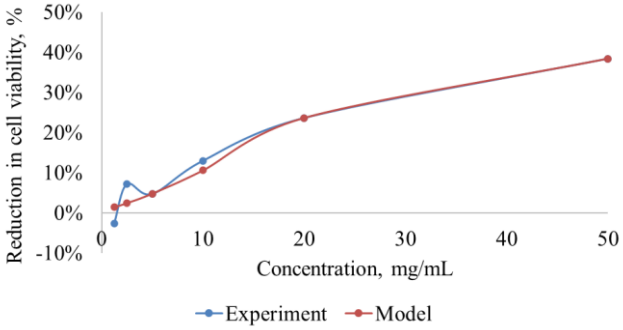

24h, 492 nm

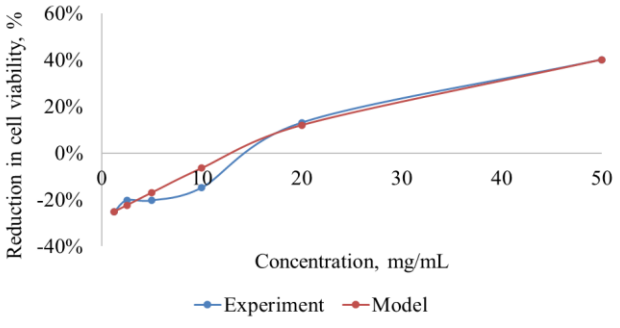

48 hours, 550 nm

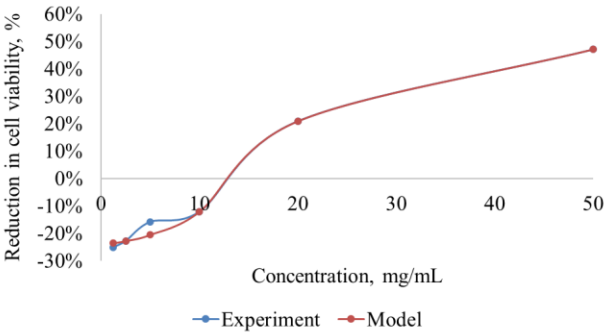

48 hours, 492 nm

Figure 6: Dynamics of T4 toxicity

All the experimental curves for T5 are in good agreement with the mathematical model, although there are slight deviations at some points. The differences between the experimental points and the model are more pronounced at 24 hours of exposure, especially at 492 nm, where emissions are observed at low concentrations. After 48 hours of exposure, the toxic effect stabilizes, and the differences between the model and the experiment become less pronounced (Fig. 7)

The results obtained for sample T6 demonstrate

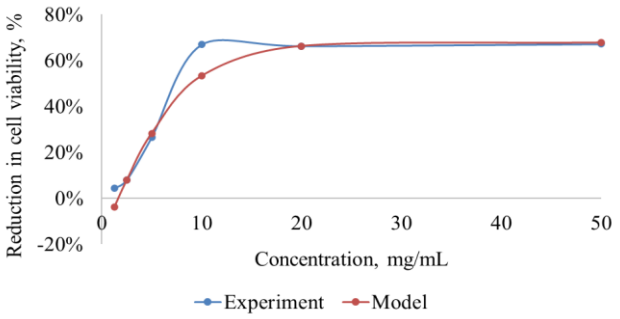

24 hours, 550 nm

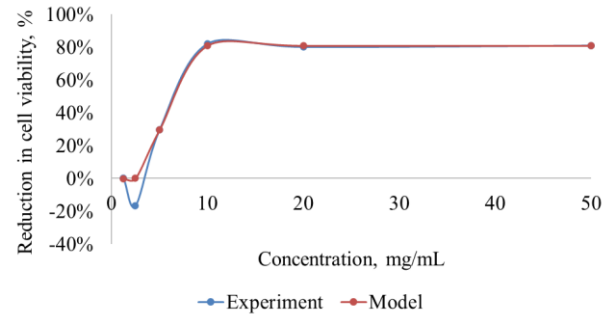

24 hours, 492 nm

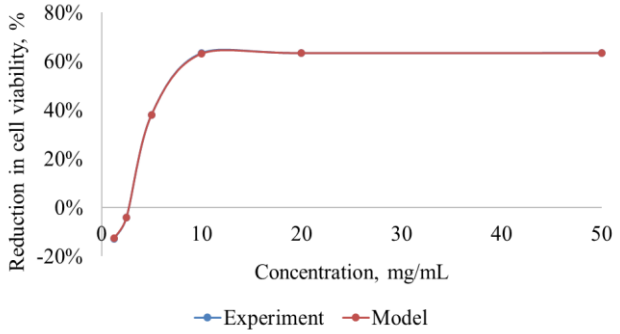

48 hours, 550 nm

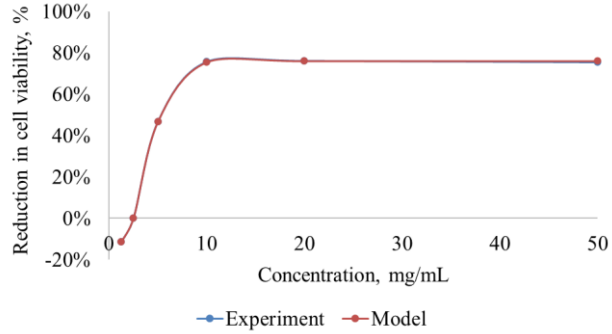

48 hours, 492 nm

Figure 7: Dynamics of T5 toxicity

a slight fluctuation in viability at low concentrations of the test compound (0–10 mg/ml) (Fig. 8). It is expected that with increasing concentration, there is a positive trend of decreasing viability, which is qualitatively described by the model. In general, the model reflects the general trends of the experimental data well. Negative values at the initial concentrations may indicate metabolic compensation of cells or the stimulatory effect of low concentrations. However, at concentrations above 20 mg/ml, the most pronounced decrease in viability is observed, indicating an increase in the toxic effect over time. The maximum toxic effect of T6 is shown at a concentration of 50 mg/ml – 31% decrease in cell viability. The absorbance values at 492 nm and 550 nm show similar patterns, which indicates the consistency of the MTT test results in both spectral ranges.

When studying the viability of HNK-21 cells under the influence of the T7 sample, significant changes in the cell monolayer and a sharp decrease in cell viability were observed in the concentration range from 10 mg/ml, after which the curve reached a plateau. This effect is clearly observed at different wavelengths and exposure times (Fig. 9), indicating a significant stability of the system.

To analyze the correspondence of the results obtained after 24 and 48 hours of exposure, a two-dimensional scatter plot was constructed (Fig. 10), which demonstrated the nonlinearity of the data obtained at different time intervals. Although this nonlinearity indicates possible complex biological mechanisms in the dynamics of the toxic effect, its level is insignificant. This makes it possible to make a practical assumption about the equality of results after 24 and 48 hours of exposure.

The results of the analysis between the measurements at 492 nm and 550 nm indicate a high correlation between the values of the percentage of viability drop measured at 550 nm and 492 nm, both after 24 hours and 48 hours of exposure, which is confirmed by high coefficients of determination ($R^2 > 0.98$) (Fig. 11). However, the nature of the regression dependencies is different: for 24 hours the slope coefficient exceeds 1 (1.22), indicating a higher sensitivity of the method at 550 nm at the early stages of cell damage, while for 48 hours the slope is less than 1 (0.82), i.e., the drop in viability recorded at 492 nm is more pronounced at a later stage. This is consistent with the mechanism of action of the MTT assay, which is based on the metabolic activity of mitochondria: in the early stages, cells are still able to reduce MTT to formazan, while with prolonged exposure to the toxicant, decreased metabolism, structural damage, or cell death cause a greater difference in the values at 492 nm. Thus, the spectrophotometric measurement at 550 nm better reflects early metabolic changes, while the measurement at 492 nm reflects later manifestations of toxicity.

When analyzing the results of the neural net work, we obtained data on the proportion of cellular area in the images, the total number of cells, and their average size for each monolayer (Table 2).

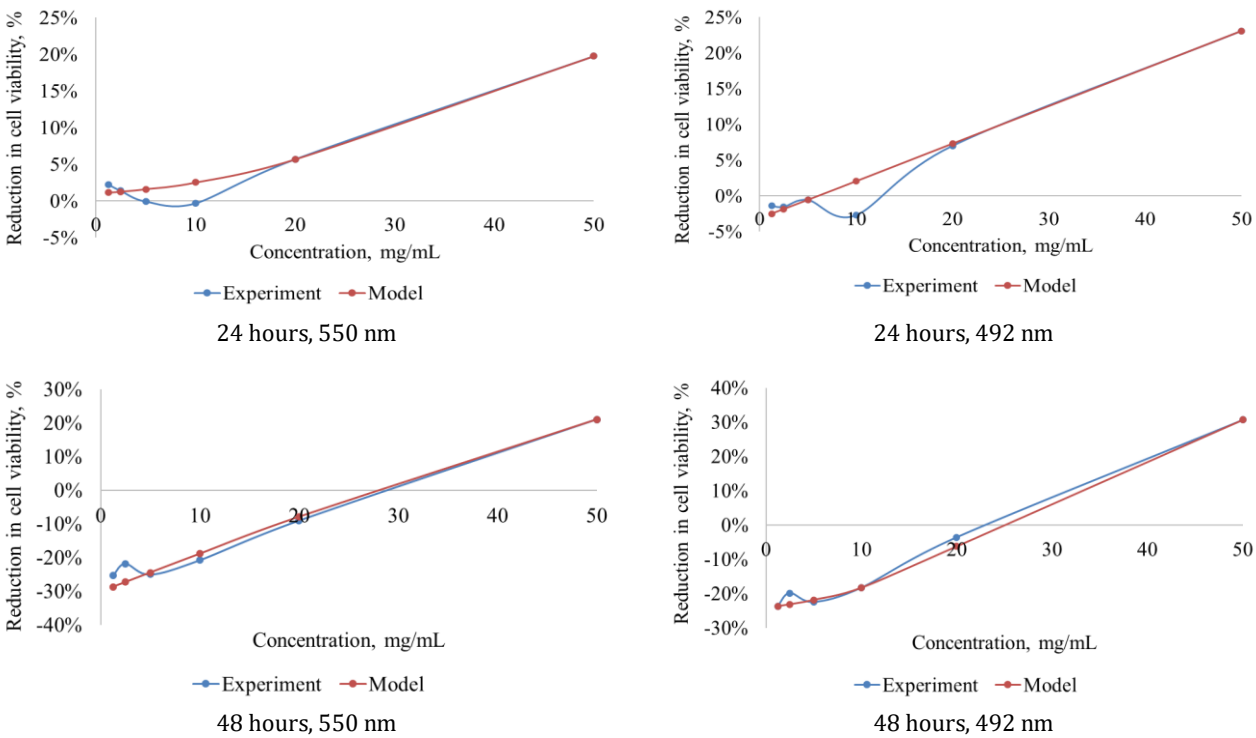

Figure 8: Dynamics of T6 toxicity

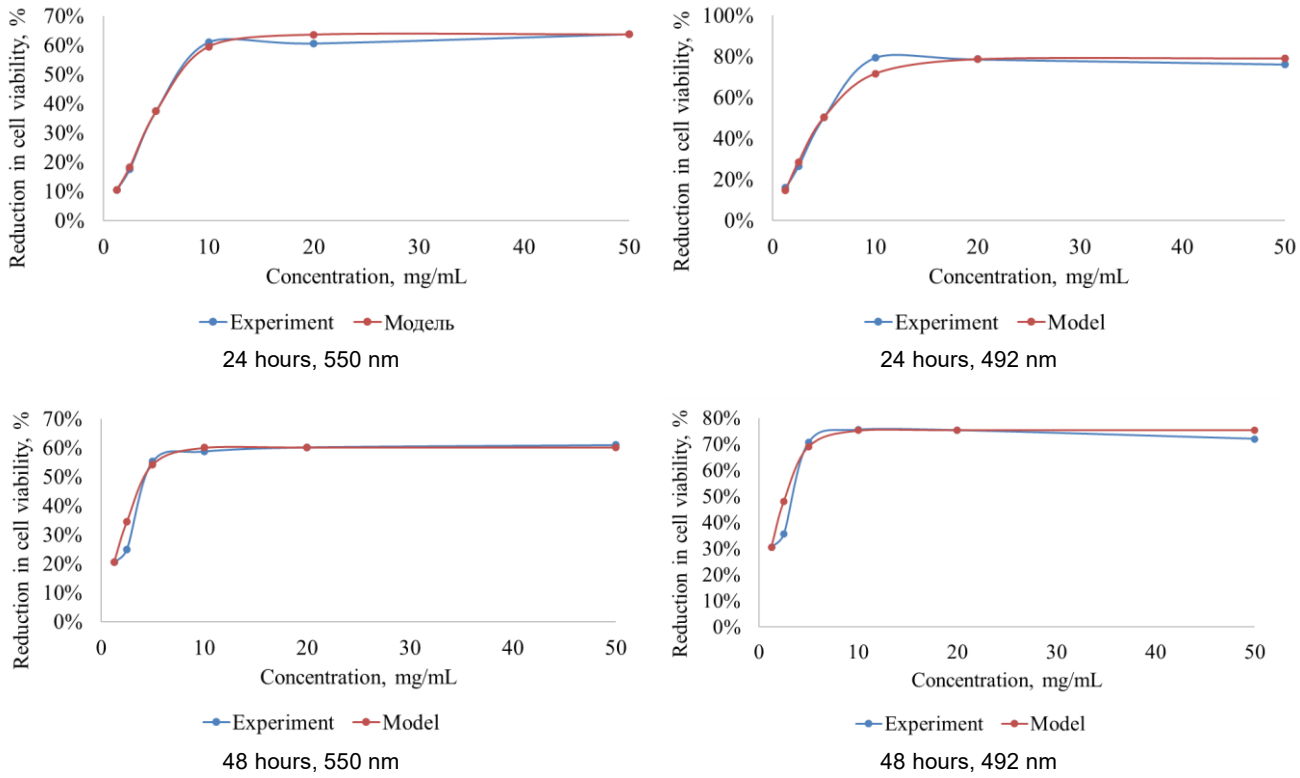

Figure 9: Dynamics of T7 toxicity

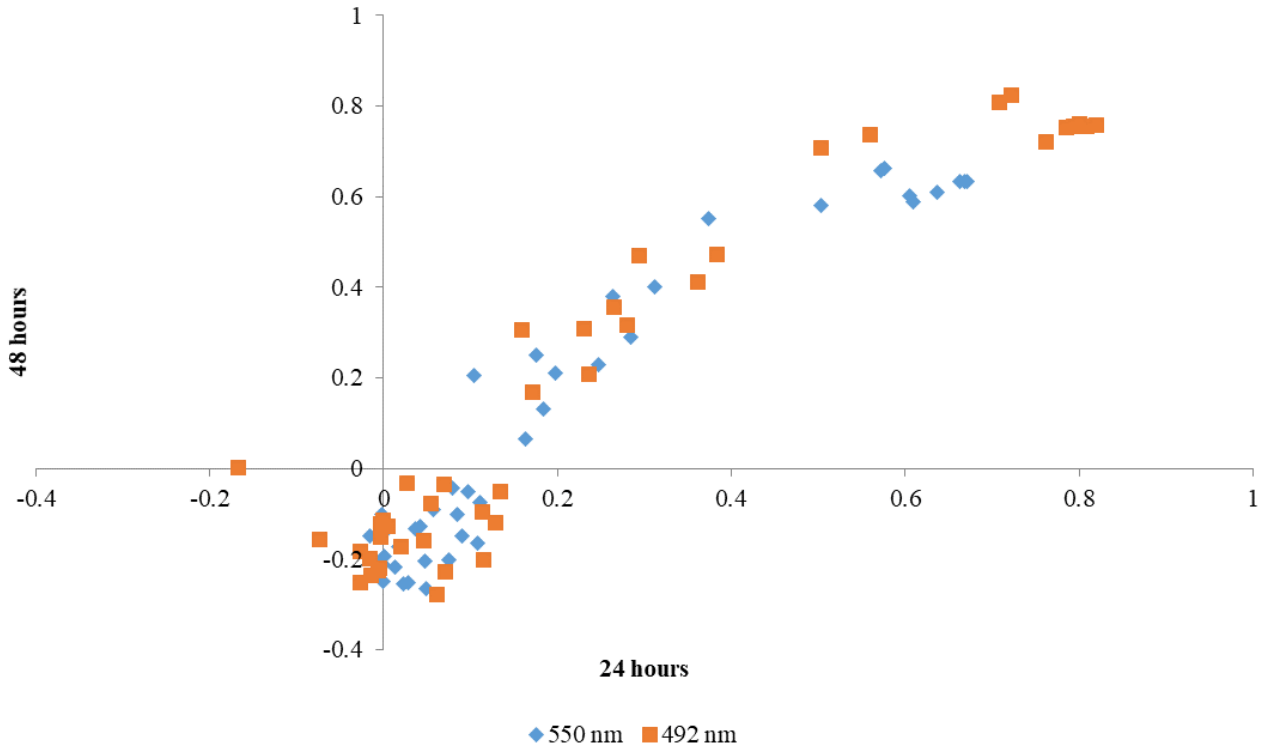

Figure 10: Analysis of the correlation between the results of viability decline in different time periods

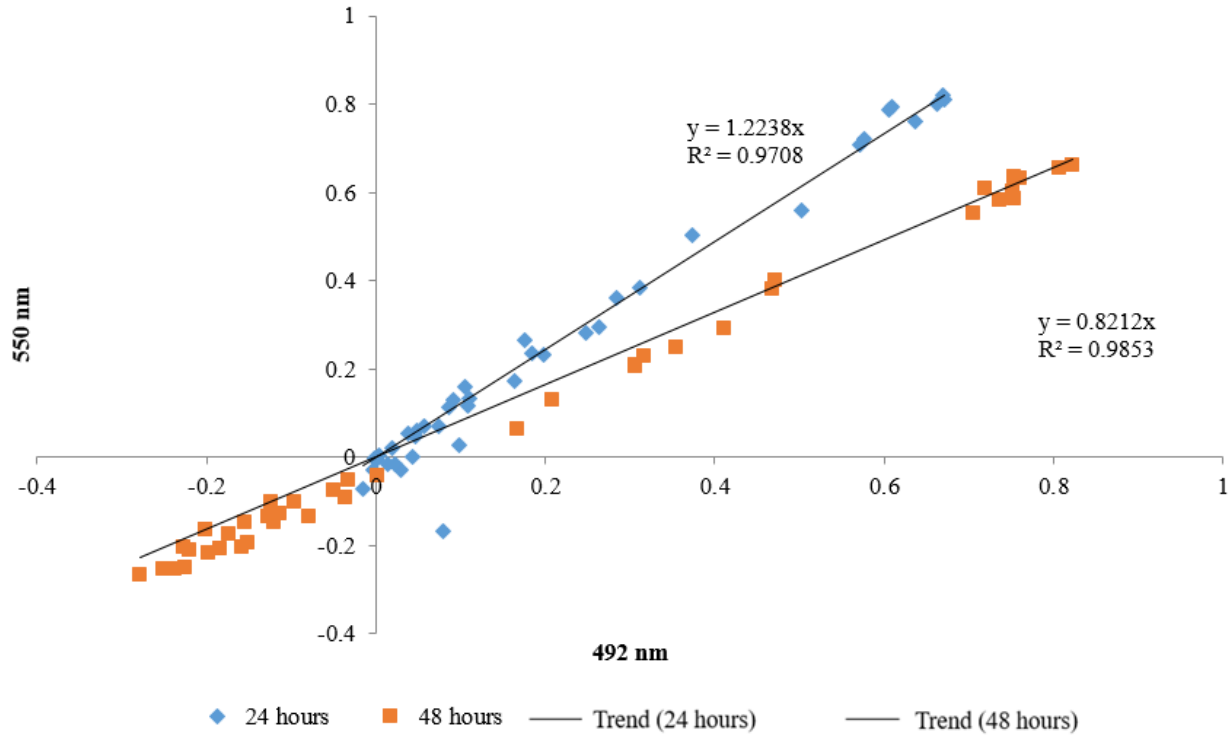

Figure 11: Correlation analysis of the results of viability drop measured at different wavelengths

The developed image-based viability assessment pipeline combines automated segmentation via Cellpose with a custom feedforward neural network to predict relative decreases in cell viability from morphological and spectrophotometric features. These metrics correspond to an effective predictive accuracy of approximately 74.7 %, or equivalently a maximum deviation of ± 25 % around the true viability reduction.

Given the limited dataset (n = 29), the allocation of a separate validation subset would further reduce the effective training sample and lead to unstable parameter estimation.

Since no validation subset was available, early stopping could not be implemented, which increases the risk of overfitting despite applied regularization. More rigorous assessment methods such as cross-validation or bootstrapping were not feasible with the present dataset size.

On the held-out test subset, the error level

Table 2: Image processing results

Test sample	Concentration, mg/ml	Calculated percentage of live cells in the image, %	Calculated number of live cells in the image, n	Cell size, pixels
Reference	0	80–89	634–681	97–102
T1	20	34–64	228–400	85
	50	24–45	163–285	75–85
T2	50	48–55	341–353	58–66
T3	5	52–56	284–347	85–100
	10	43–49	342–543	60–80
	50	59–62	183–467	60–66
T4	20	16–20	98–117	100–110
	50	13–17	146–288	50–60
T5	50	28–32	270–294	58–62
T6	10	62–66	335–386	98–101
	50	28–33	233–390	50–70
T7	1,25	10–17	295–391	50–60
	50	2–3	70–91	30–45

remained within a similar range (MAPE ≈ 28%), suggesting that the model's behaviour on these limited unseen samples does not substantially deviate from its performance on the training set. However, given the very small size of the dataset, these results should be interpreted with caution and cannot be considered a robust estimate of generalization. Importantly, by integrating quantitative measures–cell count, size, area–and spectrophotometric optical density readings into a unified feature vector, the system yields a robust, image-driven forecast of cytotoxic effect without the need for extensive manual annotation.

It is important to emphasize that evaluation based on a single 24/5 train–test split provides only a preliminary approximation of the model's generalization ability. Such a configuration, although acceptable for proof-of-concept studies, does not allow obtaining statistically robust estimates of prediction error and may underestimate the true variability of model performance on unseen data. The limitations arise directly from the specifics of in vitro cytotoxicity experiments: each measurement requires individual cultivation of cell monolayers, controlled incubation with test compounds, repeated imaging under identical optical conditions, and parallel spectrophotometric assessment. Under these constraints, collecting large, homogeneous, and reproducible image datasets is technically challenging, labor-intensive, and resource-demanding, particularly when multiple concentrations and exposure times must be evaluated simultaneously.

Discussion

In previous studies, the approximate antiviral activity of the tested compounds was evaluated under three in vitro conditions: prophylactic (compound applied 2 hours before infection), therapeutic and prophylactic (compound and virus applied simultaneously), and therapeutic (compound added 2 hours after infection). The compounds showed no preventive activity in the prophylactic mode, even at the highest concentrations (%CFD = 100%). However, under therapeutic and therapeutic-prophylactic conditions, several compounds – particularly T1, T2, T6, and T7 – demonstrated moderate to high antiviral activity, with increased efficacy at lower concentrations. The most pronounced therapeutic effect was observed for T1, T6, and T7, which significantly reduced the cytopathic effect at moderate doses [32]. A distinctive feature of the present study is the detailed time-course evaluation of compound toxicity combined with the use of information technologies for its analysis. Unlike conventional approaches, we introduced an integrated method based on automated image analysis and neural network algorithms, which enables the combined use of morphological features (cell count, area, size) anspectrophotometric MTT measurements within a single analytical framework for cytotoxicity assessment.

Given the small size of the dataset (n = 29), a meaningful comparison with baseline methods such as linear regression, decision trees, or SVR is simply not feasible. With so few samples, even the most basic models tend to behave unpredictably: their performance can fluctuate substantially from one split to another, and any apparent differences between algorithms mainly reflect the randomness of the sample rather than real differences in how well the methods work.

For this reason, we did not aim to rank or identify the "best" predictive model in this study. Instead, the neural network was used as a proof-of-concept tool to demonstrate that heterogeneous morphological and spectrophotometric data can be integrated within a single analytical framework, and that such integration may capture nonlinear patterns that simpler approaches might miss.

A direct comparison between the variability of the model's predictions and the inherent variability of the MTT assay was not performed in this study. Although four technical MTT replicates were obtained for each concentration, the model was built using only the averaged optical density values. As a result, the individual replicate measurements were not included in the modelling workflow and cannot be directly compared with the variability of the model outputs.

In addition, a reliable assessment of MTT assay variability usually requires not only technical repeats but also independent biological replicates and measurements performed across different plates or experimental runs. Such data were not available within the scope of this work. For this reason, our focus was on demonstrating the feasibility of combining morphological descriptors with spectrophotometric measurements, rather than on a detailed quantification of predictive variability relative to the intrinsic noise of the MTT assay.

The analysis of the dynamics of BHK-21 cell viability at two different wavelengths, 492 nm and 550 nm, enabled us to evaluate differences in the detection of cytotoxic effects across the test samples. Overall, cell viability values were consistently slightly lower at 550 nm compared to 492 nm. These findings indicate that classical MTT assay methods have limitations in differentiating between early and late stages of toxic exposure, which may lead to inaccuracies in identifying threshold concentrations. In contrast, the application of automated IT-based approaches allowed the detection of more subtle morphological alterations in the cell monolayer that are not always reflected by metabolic activity but may serve as critical early predictors of cytotoxicity.

After 24 hours, most of the test samples showed a similar correlation between their concentration and

cell viability at both wavelengths. Despite the presence of certain differences in the results obtained at 492 and 550 nm, the correlation trend remained. This indicates the stability and homogeneity of the results obtained.

Since the automated image processing was performed for a 24-hour exposure, a comparison of these results with the MTT assay data obtained at 24 and 48 hours demonstrated a high level of concordance. In most samples, a correlation between cell viability and compound concentration was observed at both time points, indicating the reproducibility of the results. This suggests that automated image analysis enables cytotoxicity prediction with an accuracy of approximately 75%, making it a viable alternative to classical methods at the stages of preliminary screening. Such an approach significantly reduces the duration of the study and lowers the costs associated with conducting a full-scale MTT assay.

After 48 hours of exposure, the trends recorded after 24 hours are maintained. However, for some samples (T2 and T4), the difference between the wavelengths decreased, which may indicate a stabilization of the toxic effect over time. In the case of samples where the difference between the wavelengths is maintained or even increased, it is possible to assume the presence of additional factors of influence, such as the cumulative effect of metabolites of compounds.

Different values of cell viability at different wavelengths can be due to different absorption of light by cells, as they have specific absorption spectra for each wavelength. It is also worth considering the different optical properties of cellular components, which can also change the measurement results at different wavelengths.

The time course analysis demonstrated a general increase in the toxic effect after 48 hours in all samples, indicating a cumulative effect or a gradual disruption of cellular adaptation mechanisms.

An interesting feature of the data obtained is the initial increase in cell viability at low concentrations for T1, T2, T4, and T6, which may indicate the biological activity of these compounds in a certain concentration range. This is especially clearly observed after 48 hours of exposure. For T1, this effect is likely due to the fact that GABA has antioxidant properties that can reduce oxidative stress, which has a positive effect on cell viability [44].

It is also known from the sources that GABA (T1) can act as an alternative energy source, metabolized through the GABA shunt to form succinate, which enhances mitochondrial activity and oxidative phosphorylation [45]. Given this mechanism and the experimental data obtained, it can be assumed that the presence of a GABA shunt in BHK-21 cells contributes to the increase in mitochondrial dehydrogenase activity and, accordingly, affects the MTT test result.

In general, it can be said that the studied amino carboxylic compounds have various physicochemical properties that affect their bioavailability, membrane permeability, and, as a result, potential cytotoxicity. Short-chain compounds, such as 4-aminobutyric (GABA, T1) and 5-aminovaleric acids (T2), are highly soluble in water due to their high polarity, but their permeability to lipid environments may be limited, potentially reducing their toxicity [46]. In turn, 6-aminohexanoic acid (T3) and 6-aminocaproic acid (T6) have a longer aliphatic chain, which increases their lipophilicity and biological activity [40, 47].

Medium-chain compounds, such as 7-aminoheptanoic acid (T5) and 8-aminocaprylic acid (T4), exhibit amphiphilic properties, which facilitates their interaction with biological membranes [48, 49]. T4 is particularly characterized by its ability to diffuse into lipid environments, which may affect its cytotoxic effect [50]. Methyl-6-aminocapronate hydrochloride (T7) is a modified compound with high reactivity, which improves its cell permeability and affects biological activity.

In general, an increase in carbon chain length and lipophilicity increases the ability of compounds to penetrate cell membranes, which can both contribute to therapeutic effects and increase potential cytotoxicity through interaction with membrane structures and protein complexes [50–52].

Automated image processing of the cell monolayer made it possible to assess changes in cell size, number, and relative total area in the image. In particular, the correlation between the concentration of the studied compounds and changes in cell size was the most revealing, as it indicates toxic effects that cause changes in cell morphology.

In general, it can be noted that with an increase in the concentration of the compound, a decrease in the average cell size is observed. For example, the T1 sample at a concentration of 20 mg/ml shows an average cell size of 85 pixels, and at a concentration of 50 mg/ml, the size decreases to 75–85 pixels, indicating a change in cell morphology at a higher concentration. In the T2 sample at a concentration of 50 mg/ml, the average cell size is 58-66 pixels, which is a significant decrease compared to the reference, where the average cell size varies between 97–102 pixels.

In the case of T4, no changes in cell morphology were observed at a concentration of 20 mg/ml compared to the reference, and at a concentration of 50 mg/ml, the cells shrank to 50–60 pixels, which is a clear example of how increasing the concentration of a compound can lead to a decrease in cell size, possibly due to inhibition of cell division or other metabolic changes.

The data of T3, T5 and T7 samples at concentrations of 10 mg/ml and above show that the cell size practically does not change, which indicates the stabil-

ity of cell morphology within these doses. This phenomenon correlates with the plateau effect observed in the MTT test results. When the concentration of compounds increases after a certain threshold (10 mg/ml or more), changes in cell size are not significant, and this may indicate that a level has been reached at which further increases in concentration do not lead to a proportional decrease in cell size or changes in cell morphology. Thus, the stability of cell size in these samples is consistent with the presence of a saturation effect when further exposure to the compound does not cause significant changes in the cells, which can also be observed in the results of the MTT test, where a plateau of efficacy or toxicity is reached.

With increasing concentrations of the studied compounds, there is also a general tendency to decrease both the number of cells and their relative area in the images. A decrease in the number of cells in the images also indicates a violation of cellular viability as a result of the compounds. The downward trend in the percentage of cells also correlates with the results of cytotoxicity tests, confirming the negative impact of elevated concentrations.

Thus, automated image processing is an important tool for visualizing changes in cell morphology and cell number under different exposures to the compounds under study.

It is important to understand that the MTT assay does not provide detailed information about morphological changes in cells, including changes in their shape or size, which can be an important aspect of cytotoxicity. In addition, the MTT assay only assesses the metabolic activity of cells, which may not always be a correct indicator of cell viability, as some cells may remain active but be damaged or functionally inactive. In addition, this method may be sensitive to certain chemicals that may inhibit tetrazolium reduction, distorting the results.

Instead, automated image processing does not reflect the metabolic activity of cells, as it only evaluates their physical presence and morphological changes. Also, certain algorithms may have difficulty with correct segmentation in the presence of cells with fuzzy contours and poor image quality.

Thus, the combination of image processing and the MTT assay allows for a comprehensive assessment of cytotoxicity, combining a detailed analysis of morphological changes in cells with data on their metabolic activity. This approach provides a more accurate and comprehensive characterization of the effect of the compounds under study on cell viability.

The use of artificial intelligence algorithms to analyze experimental images opens up new opportunities for automated cytotoxicity assessment, allowing not only the identification of cells and classification of them by the level of damage but also the prediction of the dynamics of toxic effects in the long term. Automated cell segmentation using neural network models allows us to effectively analyze changes in the cell monolayer under the influence of the test substances.

The results of the study confirmed that the combination of traditional methods, in particular the MTT test, with the analysis of cell morphological changes using artificial intelligence algorithms improves the interpretation of cytotoxic effects. In particular, the correlation between changes in cell area and cell viability revealed the dose-dependent nature of the toxic effect and confirmed the effect of hormesis for some samples.

In addition, the integration of artificial intelligence into the analysis process allows us to determine the threshold concentrations at which the cytotoxic effect of substances begins and calculate CD_{50}, which is a critical indicator for assessing their safety. The use of neural networks also opens up opportunities for building artificial intelligence models that can predict the potential toxic effects of new compounds based on the data obtained.

Thus, the introduction of automated cytotoxicity assays significantly improves the accuracy and reproducibility of experimental studies, reducing the subjectivity of the assessment. This, in turn, can significantly optimize the process of screening antiviral drugs, reducing the time and resources required for the development of new drugs.

To automate and preliminarily assess the cytotoxicity of the compounds under study, we employed an image processing method based on the Cellpose neural network architecture. This approach enabled rapid and objective quantification of key morphological parameters of the cell monolayer, including cell number, size, and shape – indicators that are often sensitive to cytotoxic damage but may not be fully captured by conventional biochemical assays. For this purpose, we developed custom software, CellCalc, which integrates the Cellpose model and provides automated cell detection, quantification, and estimation of the relative area of the cell monolayer in comparison with control samples.

The use of artificial intelligence for cell segmentation and predictive modeling introduced a new level of data interpretation. Compared to previously published approaches [33–35], which relied primarily on basic image processing algorithms (e.g., thresholding or edge detection), our system demonstrated significantly improved concordance between morphological metrics and biochemical test outcomes, such as MTT assay results. Moreover, the application of neural networks significantly reduced the volume of manual work, minimized user bias, and enhanced the reproducibility and scalability of cytotoxicity assessments. This methodological advancement facilitates high-throughput and standardized analysis, making it particularly valuable for drug screening and toxicit

profiling.

The neural network it brings together morphological features of the cell monolayer, quantitative measurements obtained from image segmentation, and spectrophotometric MTT readings to produce an integrated estimate of cytotoxicity. This makes it possible to account for both metabolic activity and structural changes in the cell population at the same time – an aspect that is often difficult to capture with traditional statistical models, especially when the relationships between variables are nonlinear. Because the network works with a multidimensional set of features (cell count, area, size, optical density, and others), it can approximate these interactions without relying on predefined assumptions about the form of the dependence.

Another practical advantage of this approach is the potential to use the model as an early screening tool before running a full MTT assay. Automated evaluation of morphological changes allows researchers to quickly filter out compounds that are clearly cytotoxic or unlikely to be of interest, reducing the amount of experimental work required. Collecting large and consistent in vitro datasets is technically demanding and resource-intensive, which limits the feasibility of applying more sophisticated methods at this stage. Even so, the proposed approach demonstrates the usefulness of integrating morphological and metabolic indicators and can serve as a foundation for future development of automated systems for cytotoxicity assessment.

Conclusions

A systematic analysis of the cytotoxicity of the test samples on BHK-21 cells was performed using a standard MTT assay and automated image processing. The results obtained allowed us to assess the dynamics of cell viability at different wavelengths, which made it possible to identify certain differences in the spectrophotometric determination of cell metabolic activity. Measurements performed at 550 nm demonstrated greater sensitivity in detecting early metabolic changes in cells, making this wavelength preferable for identifying subtle cytotoxic effects during initial stages of exposure. It was found that the values of cell viability at 550 nm are generally lower, which may be due to differences in the spectral characteristics of cell components. The time course analysis showed an increase in cytotoxic effects after 48 hours of exposure, which may indicate the cumulative effect of the studied compounds or a gradual disruption of cellular adaptation mechanisms. Moreover, a comparative analysis of cytotoxicity at 24 and 48 hours revealed that extending the exposure time to 48 hours did not significantly alter the overall trends in cell viability. This suggests that a 24-hour incubation period is sufficient for reliable cytotoxicity assessment, allowing for reduced assay duration without compromising result accuracy. In addition, for some samples, a hormesis effect was recorded, which is manifested in an increase in cell viability at low concentrations.

Automated image processing of the cell monolayer made it possible to assess changes in cell morphology under the influence of the test samples. A natural decrease in the average cell size with increasing concentration of compounds was found, which confirms the presence of cytotoxic effects. For some samples, a plateau effect was recorded when an increase in concentration did not cause further significant changes in cell morphology, which correlated with the results of the MTT test. In addition, there was a dose-dependent decrease in the number of cells and their percentage in the images, which is consistent with the cytotoxicity results.

The combination of the MTT assay with computer-based image analysis made it possible to obtain a more comprehensive view of the effects of the studied compounds. The developed IT tool and automated algorithms reduced the time and labor required for cytotoxicity assessment. With an approximate predictive accuracy of 75%, the proposed approach may serve as a cost-effective and reproducible complement to classical methods, particularly in preliminary or high-throughput screening of biologically active compounds.

Although the dose–response tendencies and the indications of possible hormesis observed in the dataset appear biologically reasonable, interpretations based on AI-generated predictions should be approached with some caution. The neural-network model used in this work represents an initial proof-of-concept, and its performance has been evaluated only within the constraints of the available dataset.

At the same time, this approach enables not only the estimation of cell viability but also the analysis of morphological changes, thereby expanding the possibilities for toxicity evaluation. The application of artificial intelligence to cellular image analysis demonstrates the potential for developing automated cytotoxicity screening tools that could streamline the study of biologically active compounds and support the search for new therapeutic agents.

Financing

The study has no external sources of funding.

Interests disclosure

The authors declare no conflict of interest.

References

[1] Galagan R, Andreiev S, Stelmakh N, Rafalska Y, Momot A. Automation of Polycystic Ovary Syndrome Diagnostics Through Machine Learning Algorithms in Ultrasound Imaging. Appl Comput Sci. 2024;20(2):194-204. DOI: 10.35784/acs-2024-24

[2] Mulabbi EN, Tweyongyere R, Byarugaba DK. The history of the emergence and transmission of human coronaviruses. Onderstepoort J Vet Res. 2021 Feb 10;88(1). DOI: 10.4102/ojvr.v88i1.1872

[3] Lamers MM, Haagmans BL. SARS-CoV-2 pathogenesis. Nat Rev Microbiol. 2022 May 30;20(5):270-84. DOI: 10.1038/s41579-022-00713-0

[4] Yang Y, Peng F, Wang R, Guan K, Jiang T, Xu G, et al. The deadly coronaviruses: The 2003 SARS pandemic and the 2020 novel coronavirus epidemic in China. J Autoimmun. 2020 May; 10(9):1024-34. DOI: 10.1016/j.jaut.2020.102434

[5] Zaki AM, van Boheemen S, Bestebroer TM, Osterhaus ADME, Fouchier RAM. Isolation of a Novel Coronavirus from a Man with Pneumonia in Saudi Arabia. N Engl J Med. 2012 Nov 8;367(19):1814-20. DOI: 10.1056/NEJMoa1211721

[6] Al-Rohaimi AH, Al Otaibi F. Novel SARS-CoV-2 outbreak and COVID-19 disease; a systematic review on the global pandemic. Genes Dis. 2020 Dec;7(4):491-501. DOI: 10.1016/j.gendis.2020.06.004

[7] Peng XL, Cheng JSY, Gong HL, Yuan MD, Zhao XH, Li Z, et al. Advances in the design and development of SARS-CoV-2 vaccines. Mil Med Res. 2021 Dec 16;8(1):67. DOI: 10.1186/s40779-021-00360-1

[8] Cosar B, Karagulleoglu ZY, Unal S, Ince AT, Uncuoglu DB, Tuncer G, et al. SARS-CoV-2 Mutations and their Viral Variants. Cytokine Growth Factor Rev. 2022 Feb; 63:10-22. DOI: 10.1016/j.cytogfr.2021.06.001

[9] Tan CCS, Lam SD, Richard D, Owen CJ, Berchtold D, Orengo C, et al. Transmission of SARS-CoV-2 from humans to animals and potential host adaptation. Nat Commun. 2022 May 27;13(1):2988. DOI: 10.1038/s41467-022-30698-6

[10] Fichtner M, Voigt K, Schuster S. The tip and hidden part of the iceberg: Proteinogenic and non-proteinogenic aliphatic amino acids. Biochim Biophys Acta - Gen Subj. 2017 Jan;1861(1):3258-69. DOI: 10.1016/j.bbagen.2016.08.008

[11] Skwarecki AS, Nowak MG, Milewska MJ. Amino Acid and Peptide-Based Antiviral Agents. ChemMedChem. 2021 Oct 15;16(20):3106-35. DOI: 10.1002/cmdc.202100397

[12] Avrahami D, Oren Z, Shai Y. Effect of Multiple Aliphatic Amino Acids Substitutions on the Structure, Function, and Mode of Action of Diastereomeric Membrane Active Peptides. Biochemistry. 2001 Oct 1;40(42):12591-603. DOI: 10.1021/bi0105330

[13] Luiking YC, Deutz NEP. Biomarkers of Arginine and Lysine Excess. J Nutr. 2007 Jun;137(6):1662S-1668S. DOI: 10.1093/jn/137.6.1662S

[14] Mailoo VJ, Rampes S. Lysine for Herpes Simplex Prophylaxis: A Review of the Evidence. Integr Med (Encinitas). 2017 Jun;16(3):42-6.

[15] Dziublyk I, Soloviov S, Trokhimenko O, Dziublyk O, Smetiukh M, Yakovenko O, et al. In vitro study of the spectrum of antiviral activity of aliphatic acid against the prototype coronavirus strain. Biomed Biotechnol Res J. 2023;7(2):218. DOI:10.4103/bbrj.bbrj_36_23

[16] S. P. Toxicological screening. J Pharmacol Pharmacother. 2011 Jun 1;2(2):74-9. DOI: 10.4103/0976-500X.81895

[17] Borenfreund E, Babich H. In vitro cytotoxicity of heavy metals, acrylamide, and organotin salts to neural cells and fibroblasts. Cell Biol Toxicol. 1987 Mar;3(1):63-73. DOI: 10.1007/BF00117826

[18] Aslantürk ÖS. In Vitro Cytotoxicity and Cell Viability Assays: Principles, Advantages, and Disadvantages. In: Genotoxicity - A Predictable Risk to Our Actual World. InTech; 2018. DOI: 10.5772/intechopen.71923

[19] Edwards V, Markovic E, Matisons J, Young F. Development of an in vitro reproductive screening assay for novel pharmaceutical compounds. Biotechnol Appl Biochem. 2008 Oct 23;51(2):63-71. DOI: 10.1042/BA20070223

[20] Astashkina A, Mann B, Grainger DW. A critical evaluation of in vitro cell culture models for high-throughput drug screening and toxicity. Pharmacol Ther. 2012 Apr;134(1):82-106. DOI: 10.1016/j.pharmthera.2012.01.001

[21] O'Brien P, Haskins JR. In Vitro Cytotoxicity Assessment. In: High Content Screening. New Jersey: Humana Press; p. 415-426. DOI: 10.1385/1-59745-217-3:415

[22] Schoonen WGEJ, Westerink WMA, de Roos JADM, Débiton E. Cytotoxic effects of 100 reference compounds on Hep G2 and HeLa cells and of 60 compounds on ECC-1 and CHO cells. I Mechanistic assays on ROS, glutathione depletion and calcein uptake. Toxicol Vitr. 2005 Jun;19(4):505-16. DOI: 10.1016/j.tiv.2005.01.003

[23] A. Momot, M. Zaboluieva RG. Automated segmentation of ultrasound medical images using the Attention U-Net model. Nor J Dev Int Sci. 2024;№128.:56-60.

[24] Mirajkar G, Garg L, Alaragisamy M, Shinde S. Image Processing in Toxicology: A Systematic Review. 2024.:159-75. DOI: 10.1007/978-3-031-72284-4_10

[25] Rajpoot K, Panchal M, Pawar B, Vasdev N, Gupta T, Tekade M, et al. High-throughput screening in toxicity assessment. In: Public Health and Toxicology Issues Drug Research, Volume 2. Elsevier; 2024.:407-49. DOI: 10.1016/B978-0-443-15842-1.00017-X

[26] Prajapati P, Shrivastav P, Prajapati J, Prajapati B. Deep Learning Approaches for Predicting Bioactivity of Natural Compounds. Nat Prod J. 2025 Jan 10;15. DOI: 10.2174/0122103155332267241122143118

[27] Naghizadeh A, Tsao W chung, Hyun Cho J, Xu H, Mohamed M, Li D, et al. In vitro, machine learning-based CAR T immunological synapse quality measurements correlate with patient clinical outcomes. Faeder JR, editor. PLOS Comput Biol. 2022 Mar 18;18(3):e1009883. DOI: 10.1371/journal.pcbi.1009883

[28] PubChem. 4-Aminobutyric Acid. Bethesda (MD): National Library of Medicine (US), National Center for Biotechnology Information; 2004–. Available from: https://pubchem.ncbi.nlm.nih.gov/compound/4-Aminobutyric-Acid

[29] PubChem. 5-Aminovaleric acid . Bethesda (MD): National Library of Medicine (US), National Center for Biotechnology Information; 2004. Available from: https://pubchem.ncbi.nlm.nih.gov/compound/5-Aminovaleric-acid

[30] PubChem. 6-Aminohexanoic Acid. Bethesda (MD): National Library of Medicine (US), National Center for Biotechnology Information; 2004. Available from: https://pubchem.ncbi.nlm.nih.gov/compound/6-Aminohexanoic-Acid

[31] PubChem. 7-Aminoheptanoic acid. Bethesda (MD): National Library of Medicine (US), National Center for Biotechnology Information; 2004–. Available from: https://pubchem.ncbi.nlm.nih.gov/compound/7-Aminoheptanoic-acid

[32] Smetiukh MP. BIOTECHNOLOGICAL SYSTEM FOR THE SEARCH OF SUBSTANCES WITH POTENTIAL ACTIVITY AGAINST CORONAVIRUS. Biotechnol Acta. 2024 Dec 16;17(6):45-55. DOI: 10.15407/biotech17.06.045

[33] Kamiloglu S, Sari G, Ozdal T, Capanoglu E. Guidelines for cell viability assays. Food Front. 2020 Sep 16;1(3):332-49. DOI: 10.1002/fft2.44

[34] Terry Riss, PhD, Andrew Niles, MS, Rich Moravec, BS, Natashia Karassina, MS, and Jolanta Vidugiriene P. Cytotoxicity Assays: In Vitro Methods to Measure Dead Cells\ 2019.
[35] Ghasemi M, Liang S, Luu QM, Kempson I. The MTT Assay: A Method for Error Minimization and Interpretation in Measuring Cytotoxicity and Estimating Cell Viability. 2023. 15-33. DOI: 10.1007/978-1-0716-3052-5_2.
[36] Tolosa L, Donato MT, Gómez-Lechón MJ. General Cytotoxicity Assessment by Means of the MTT Assay. In 2015. p. 333-48. DOI: 10.1007/978-1-4939-2074-7_26
[37] Ghasemi M, Turnbull T, Sebastian S, Kempson I. The MTT Assay: Utility, Limitations, Pitfalls, and Interpretation in Bulk and Single-Cell Analysis. Int J Mol Sci. 2021 Nov 26;22(23):12827. DOI: 10.3390/ijms222312827
[38] Mosmann T. Rapid colourimetric assay for cellular growth and survival: Application to proliferation and cytotoxicity assays. J Immunol Methods. 1983 Dec;65(1-2):55-63. DOI: 10.1016/0022-1759(83)90303-4
[39] Stone V, Johnston H, Schins RPF. Development of in vitro systems for nanotoxicology: methodological considerations. Crit Rev Toxicol. 2009 Aug 3;39(7):613-26. DOI: 10.1080/10408440903120975
[40] Supino, R. (1995). MTT Assays. In: O'Hare, S., Atterwill, C.K. (eds) In Vitro Toxicity Testing Protocols. Methods in Molecular Biology™, vol 43. Humana Press. DOI: 10.1385/0-89603-282-5:137
[41] Berridge MV, Tan AS. Characterization of the cellular reduction of 3-(4,5-dimethylthiazol-2-yl)-2,5-diphenyltetrazolium bromide (MTT): subcellular localization, substrate dependence, and involvement of mitochondrial electron transport in MTT reduction. Arch Biochem Biophys. 1993 Jun;303(2):474-82. DOI: 10.1006/abbi.1993.1311.
[42] Aslantürk Ö, Çelik T, Karabey B, Karabey F. Active Phytochemical Detection, Antioxidant, Cytotoxic, Apoptotic Activities of Ethyl Acetate and Methanol Extracts of Galium aparine L. Br J Pharm Res. 2017 Jan 10;15(6):1-16. DOI: 10.9734/BJPR/2017/32762
[43] Zhang M, Aguilera D, Das C, Vasquez H, Zage P, Gopalakrishnan V, et al. Measuring cytotoxicity: a new perspective on LC50. Anticancer Res. 2007;27(1A):35-8.
[44] Hou D, Tang J, Feng Q, Niu Z, Shen Q, Wang L, et al. Gamma-aminobutyric acid (GABA): A comprehensive review of dietary sources, enrichment technologies, processing effects, health benefits, and its applications. Crit Rev Food Sci Nutr. 2024 Sep 20;64(24):8852-74. DOI: 10.1080/10408398.2023.2204373
[45] Cavalcanti-de-Albuquerque JP, De-Souza-Ferreira E, de Carvalho DP, Galina A. Coupling of GABA Metabolism to Mitochondrial Glucose Phosphorylation. Neurochem Res. 2022 Feb 8;47(2):470-80. DOI: 10.1007/s11064-021-03463-2
[46] Lee XY, Tan JS, Cheng LH. Gamma Aminobutyric Acid (GABA) Enrichment in Plant-Based Food - A Mini Review. Food Rev Int. 2023 Sep 8;39(8):5864-85. DOI: 10.1080/87559129.2022.2097257
[47] Ooka AA, Kuhar KA, Cho N, Garrell RL. Surface interactions of a homologous series of alpha,omega-amino acids on colloidal silver and gold. Biospectroscopy. 1999;5(1):9-17. DOI: 10.1002/(SICI)1520-6343(1999)5:1<9::AID-BSPY3>3.0.CO;2-T
[48] National Center for Biotechnology Information. 7-Aminoheptanoic acid hydrochloride. 2025. Available from: https://pubchem.ncbi.nlm.nih.gov/compound/7-Aminoheptanoic-acid-hydrochloride
[49] PubChem. 8-Aminocaproic acid. Bethesda (MD): National Library of Medicine (US). Available from: https://pubchem.ncbi.nlm.nih.gov/compound/8-Aminocaproic-acid
[50] Nandi N, Gayen K, Ghosh S, Bhunia D, Kirkham S, Sen SK, et al. Amphiphilic Peptide-Based Supramolecular, Noncytotoxic, Stimuli-Responsive Hydrogels with Antibacterial Activity. Biomacromolecules. 2017 Nov 13;18(11):3621-9. DOI: 10.1021/acs.biomac.7b01006
[51] Morimoto J, Sando S. Development and Application of Methodologies for Measuring Passive Membrane Permeability of Peptides toward Understanding the Structure-permeability Relationship of Cyclic Peptides. J Synth Org Chem Japan. 2024 Jun 1;82(6):613-21. DOI: 10.5059/yukigoseikyokaishi.82.613
[52] Steigenberger J, Verleysen Y, Geudens N, Martins JC, Heerklotz H. The Optimal Lipid Chain Length of a Membrane-Permeabilizing Lipopeptide Results From the Balance of Membrane Partitioning and Local Damage. Front Microbiol. 2021 Sep 14;12. DOI: 10.3389/fmicb.2021.669709

М.П. Сметюх[1*], А.С. Момот[1], О.П. Трохименко[2], С.О. Соловйов[1,2], І. С. Даценко[2], О.К. Яковенко[3,4], Я.О. Дзюблик[5], О.В. Козир[1], М.С. Хакім[6]

[1] КПІ ім. Ігоря Сікорського, Київ, Україна
[2] Національний університет охорони здоров'я України ім. П.Л. Шупика, Київ, Україна
[3] КП «Волинська обласна клінічна лікарня», Луцьк, Україна
[4] Волинський національний університет ім. Лесі Українки, Луцьк, Україна
[5] Національний науковий центр фтизіатрії, пульмонології та алергології ім. Ф. Г. Яновського Національної академії медичних наук України, Київ, Україна
[6] Університет Кассім, Бурайда, Саудівська Аравія

ОЦІНКА ЦИТОТОКСИЧНОСТІ АЛІФАТИЧНИХ АМІНОКАРБОНОВИХ СПОЛУК ЯК ПОТЕНЦІЙНИХ ПРОТИКОРОНАВІРУСНИХ АГЕНТІВ

Проблематика. Попри успіхи у створенні вакцин проти SARS-CoV-2, висока мутагенність коронавірусів, міжвидова передача та поява нових штамів вимагають подальшого пошуку ефективних противірусних засобів. Ключовим етапом у цьому процесі є оцінка цитотоксичності потенційних сполук, що дозволяє визначити їхню безпеку та терапевтичну перспективність. Сучасні ІТ-рішення, зокрема автоматизований аналіз зображень і штучний інтелект, підвищують точність та об'єктивність оцінок.
Мета. Визначити цитотоксичність сполук із потенційною антикоронавірусною активністю та провести її аналіз із використанням ІТ-засобів.
Методика реалізації. У дослідженні використано перещеплювальну клітинну лінію ВНК-21 сірійського хом'ячка, яку інкубували з сімома аліфатичними амінокарбоновими сполуками в шести концентраціях. Життєздатність клітин визначали за допомогою

МТТ-тесту. Для автоматизованого аналізу використовували обробку зображень клітинного моношару та експоненційну модель дозозалежної відповіді.
Результати. Дослідження виявило виражену дозо- та часозалежну цитотоксичність більшості зразків, із максимальним зниженням життєздатності при концентраціях понад 10 мг/мл. Зафіксовано ефект гормезису на низьких концентраціях (до 5–10 мг/мл), що може свідчити про активацію клітинних захисних механізмів. Висока кореляція між вимірюваннями при 492 нм та 550 нм ($R^2 > 0,98$) підтвердила достовірність спектрофотометричних даних. Експоненційна модель дозволила апроксимувати криві токсичності, особливо у середньому та високому діапазонах концентрацій. Побудована нейронна мережа на основі даних зображень та МТТ-тесту показала здатність прогнозувати життєздатність клітин навіть за обмеженої кількості навчальних даних.
Висновки. Поєднання МТТ-тесту з автоматизованим аналізом зображень забезпечує комплексну оцінку цитотоксичності. Встановлено дозозалежне зниження життєздатності клітин та морфологічні зміни під впливом досліджуваних сполук. Вимірювання при 550 нм виявились більш чутливими до ранніх змін метаболізму клітин. Використання ІТ-алгоритмів продемонструвало перспективність автоматизованого підходу до скринінгу біологічно активних речовин.

Ключові слова: цитотоксичність; *in vitro*; амінокарбонові сполуки; МТТ-тест; обробка зображень; нейронна мережа.